

# Using Curvature Information in Shape Analysis

John T. Kent<sup>1</sup>, Delman Lee<sup>1</sup>, Kanti V. Mardia<sup>1</sup> and Alf D. Linney<sup>2</sup>

<sup>1</sup>Department of Statistics, University of Leeds, Leeds LS2 9JT, UK

<sup>2</sup>Department of Medical Physics, University College London, London, UK

## Abstract

Ridge curves are important features in human face. These curves are based on third derivatives of a surface in  $\mathbb{R}^3$ . Thus, they are very sensitive to noise in a discrete representation of the surface. In this paper we look at local smoothing methods to stabilize the calculation of ridge curves. An example is given using three sets of laser range data of the human head.

## 1 Introduction

The description of the surface of an object in three dimensional space can be described in terms of landmarks (identifiable points on the surface), tangent directions (first derivative information), curvatures (second derivative information), and changes in curvature (third derivative information). An example of this last type of description is given by ridge curves which represent extreme values of principal curvatures along principal curves. The purpose of this paper is to investigate the calculation of ridge curves. In general the calculation of derivative information is very susceptible to noise in the representation of a surface. Therefore, smoothing is essential in practice for the calculation of derivatives. Thus, in practice the concept of a “derivative” should be replaced by a “derivative at a particular scale”.

A simple ridge criterion given in Kent *et al.* (1996) is used to identify the location of ridge points. The ridge points are connected together to form ridge curves using a zero crossing algorithm.

The use of smoothing serves two purposes. First, it helps to remove small-scale noise in the image. Second, it removes small-scale features in the image in order to focus on larger scale features. An example might be a dimple in the chin of a human face. By smoothing over the dimple we are able to focus on the larger scale structure of the chin.

In Kent *et al.* (1996) a fitted surface based on kriging, a method related to thin plate splines, was used to carry out the smoothing necessary to calculate third order derivatives. In this paper some further investigation of their methodology is carried out. Also some other smoothing methods are briefly sketched. Finally, some examples are given using laser range data of the human face.

## 2 Definition of ridge curves

In this section we give a brief review of the mathematical description of ridge curves. First, recall that any surface can be represented, at least locally, in “parametric form”,

$$z = f(x, y), \quad (2.1)$$

with respect to a suitable coordinate system. Before defining ridge curves it is necessary to set up two preliminary concepts, the tangent plane at a point on the surface and the principal directions in this tangent plane. (See e.g. Porteous (1994) for more details.)

The tangent plane at a point  $(x, y)$  is spanned by the two vectors

$$\mathbf{u} = \begin{bmatrix} 1 \\ 0 \\ f_x \end{bmatrix}, \mathbf{v} = \begin{bmatrix} 0 \\ 1 \\ f_y \end{bmatrix}.$$

Here  $f_x = \partial f / \partial x$ , etc. Thus, a two dimensional vector  $\mathbf{p} = (p_1, p_2)^T$  defines a three-dimensional vector

$$p_1 \mathbf{u} + p_2 \mathbf{v} \quad (2.2)$$

in the tangent space.

For each such vector  $\mathbf{p}$ , the vectors  $p_1 \mathbf{u} + p_2 \mathbf{v}$  and  $[0, 0, 1]^T$  define a plane in  $\mathbb{R}^3$ . The intersection of this plane with the original surface  $z = f(x, y)$  defines a plane curve. The curvature of this curve at the point  $(x, y)$  varies with  $\mathbf{p}$ . The directions on the surface at which this curvature is extremal are called principal directions and the corresponding curvatures are called the principal curvatures. The principal directions and curvatures can be found from the (right) eigenvectors and eigenvalues of the matrix  $A^{-1}B$  where

$$A = \begin{bmatrix} 1 + f_x^2 & f_x f_y \\ f_x f_y & 1 + f_y^2 \end{bmatrix} \quad (2.3)$$

is the “matrix of the first fundamental form” and

$$B = (1 + f_x^2 + f_y^2)^{-\frac{1}{2}} \begin{bmatrix} f_{xx} & f_{xy} \\ f_{xy} & f_{yy} \end{bmatrix} \quad (2.4)$$

is the “matrix of the second fundamental form”. Points at which the two eigenvalues are equal are known as “umbilic points”. An eigenvector  $\mathbf{p}$  of  $A^{-1}B$  determines a principal direction through (2.2).

Fix a point  $(x_0, y_0, z_0)$  on the surface and suppose the coordinate system has been rotated so that in the representation (2.1) the first partial derivatives vanish,  $f_x = f_y = 0$  at  $(x_0, y_0)$ . Such a representation is known as “Monge form” at  $(x_0, y_0)$  and leads to a simplification in the matrices  $A$  and  $B$ . Thus  $A$  reduces to the identity matrix and  $B$  reduces to the matrix of second order derivatives at  $(x_0, y_0)$ . In this case the principal curvatures are given by the eigenvalues of  $B$  and the principal directions are determined by the corresponding eigenvectors of  $B$ . In other words we can think of the surface (2.1) as looking locally like a quadratic function,

$$z = z_0 + (\mathbf{t} - \mathbf{t}_0)^T B (\mathbf{t} - \mathbf{t}_0) + O(\|\mathbf{t} - \mathbf{t}_0\|^3), \quad (2.5)$$

where  $\mathbf{t} = (x, y)^T$ ,  $\mathbf{t}_0 = (x_0, y_0)^T$ . Monge form is particularly convenient for studying the surface at a single point  $(x_0, y_0)$  but is less convenient when we want to look simultaneously at the surface at several points. The reason is that a coordinate system which yields Monge form at a particular point  $(x_0, y_0)$  would not generally yield Monge form at another point on the surface. It should be noted that the eigenvalues of  $A^{-1}B$  and the directions in  $\mathbb{R}^3$  determined by the corresponding eigenvectors do not depend on which coordinate system is used to describe the surface. By a change of coordinate system we mean rotating the coordinate system to

$$\begin{bmatrix} x' \\ y' \\ z' \end{bmatrix} = G \begin{bmatrix} x \\ y \\ z \end{bmatrix} \quad (2.6)$$

where  $G$  is orthogonal, and describing the surface by  $z' = f'(x', y')$  in a neighbourhood of  $(x'_0, y'_0, z'_0)$ .

“Principal curves” on the surface are curves whose tangent directions always point in a principal direction. There are two principal curves passing through each non-umbilic point, corresponding to the larger and smaller eigenvalues of  $A^{-1}B$ , respectively. Thus, there are two families of principal curves on the surface. At each non-umbilic point these curves cross at right angles to one another.

Along a principal curve, the value of the corresponding principal curvature varies, and at certain points it has a local extremum. Such points are called “ridge points” and the set of all such points forms a collection of curves called “ridge curves”. There are two sets of curves, one for the larger and one for the smaller eigenvalue of  $A^{-1}B$ . Further, each ridge point can be classified according to whether the curvature is maximal or minimal. Let  $\mathbf{p} = (p_1, p_2)^T$  denote an eigenvector of  $A^{-1}B$  at a point  $(x, y)$  with corresponding eigenvalue  $\kappa_p$ . It can be shown that the derivative of the principal curvature  $\kappa_p$  at  $(x, y)$  along the principal curve defined by the eigenvector  $\mathbf{p}$  is given by

$$\begin{aligned} R(x, y) = & (1 + f_x^2 + f_y^2)^{-\frac{1}{2}} (p_1^3 f_{xxx} + 3p_1^2 p_2 f_{xxy} + 3p_1 p_2^2 f_{xyy} + p_2^3 f_{yyy}) \\ & - 3(p_1^2 f_{xx} + 2p_1 p_2 f_{xy} + p_2^2 f_{yy})(p_1 f_x + p_2 f_y) \kappa_p. \end{aligned} \quad (2.7)$$

In this formula the eigenvector  $\mathbf{p}$  must be standardized so that the three dimensional vector

$$(p_1, p_2, p_1 f_x + p_2 f_y)^T \quad (2.8)$$

is a unit vector. Setting  $R(x, y) = 0$  defines a set of curves in the  $(x, y)$  plane, which when projected up to the surface in  $\mathbb{R}^3$  give the ridge curves on the surface.

The formula for  $R(x, y)$  takes a particularly simple form at a point  $(x, y)$  when Monge form is used at  $(x, y)$ . In this case  $f_x = f_y = 0$ . If we also rotate the coordinates in the  $(x, y)$  plane so that the eigenvector  $\mathbf{p}$  points along the positive  $x$ -axis, then  $\mathbf{p} = (1, 0)$  with the required standardization (2.8), and (2.7) reduces to

$$R(x, y) = f_{xxx}. \quad (2.9)$$

It should be noted that the formula in (2.7) is invariant under orthogonal changes in the coordinate system. In particular, if we rotate from one coordinate system  $(x, y, z)$  to a new coordinate system as in (2.6), then the value of (2.7) remains unchanged.

A rescaled version of the formula (2.7) was used in Kent *et al.* (1996). However, the version used here has the advantage that it represents the actual derivative of principal curvature with respect to arc length as we move along a principal curve, and therefore it remains invariant under changes in the coordinate system.

### 3 Smoothing

In order to calculate the ridgeness criterion  $R$  and principal directions at a grid of points, the derivatives up to order 3 of  $f$  in (2.1) are needed. Assuming  $f$  is provided at (another) set of grid points, some sort of smoothing procedure is required. Here we review several possible approaches.

#### 3.1 Global Smoothing methods

Assume the whole surface can be given a simple parametric representation (2.1). Then a global method can be used for smoothing. One such method was used by Kent *et al.* (1996) based on kriging. Given data  $z_j$  at points  $\mathbf{t}_j = (x_j, y_j)^T, j = 1, \dots, n$ , the fitted surface takes the form

$$\hat{f}(\mathbf{t}) = P(\mathbf{t}) + \sum_{j=1}^n \beta_j \sigma(\mathbf{t} - \mathbf{t}_j)$$

where  $P(\mathbf{t})$  is a polynomial in  $\mathbf{t}$  and  $\sigma(\cdot)$  is a suitable conditionally positive definite “potential” function. In the application of that paper the choice  $\sigma(\mathbf{t}) = -\|\mathbf{t}\|^5$  was used and  $P(\mathbf{t})$  was a polynomial of degree 2. The coefficients  $\beta_j$  satisfied the constraints  $\sum \beta_j t_{j1}^{\alpha_1} t_{j2}^{\alpha_2} = 0$  for  $\alpha_1, \alpha_2 \geq 0, \alpha_1 + \alpha_2 \leq 2$ . This choice was used to ensure that the third derivatives of the fitted surface  $\hat{f}(x, y)$  exist and are smooth. The kriging predictor can be formulated as a predictor for a certain spatial stochastic process with a specified covariance and drift structure, given data at  $\mathbf{t}_j, j = 1, \dots, n$ . See, e.g. Mardia *et al.* (1996) for a more detailed description. The method includes a smoothing parameter which controls the trade-off between fidelity to the data and smoothness.

Although the kriging method yields useful visualizations of ridge curves, there are also some drawbacks. To use the kriging methodology it is necessary to represent the surface in parametric form,  $z = f(x, y)$ . Such a representation can always be given locally but may not be possible globally. Further, it is necessary to pick out a set of  $n$  landmarks on the surface which give an approximate description of the surface. If  $n$  landmarks are used the kriging methodology involves the inversion of an  $n \times n$  matrix, which is an operation requiring  $O(n^3)$  mathematical calculations. Thus, it is necessary to limit the number of landmarks in practice. Kent *et al.* (1996) used  $n = 200$  points. Further, unless smoothing is carried out, the position and value of the surface of these landmarks can have a noticeable effect on the kriging solution.

For data on a regular grid it may be possible to greatly increase the size of  $n$  for the same computational burden by using a tensor product of one-dimensional splines. See e.g. Guéziec (1995) for related work.

## 3.2 Local regression

We need to calculate the third derivatives of  $f(x, y)$  in (2.1) with respect to  $x$  and  $y$ . As noted in equation (2.9) these derivatives are most closely linked to the definition of ridge curves when the coordinate system is close to Monge form. Therefore, we shall investigate the following procedure to calculate smoothed versions of these derivatives. Similar ideas were suggested by Flynn and Jain (1989).

First, choose a point on the surface. Second, choose a neighbourhood of points close to the given point, e.g. all points within a distance  $r$ , say, of the given point. Next, carry out a principal component analysis in  $\mathbb{R}^3$  of all the points in this window. Since the surface will be locally flat in a small neighbourhood of a given point, the principal component analysis should yield the following results. The first two eigenvalues should be much larger than the third eigenvalue which should be near zero. Further, the corresponding eigenvectors should approximately lie in the tangent space to the surface at this given point. (See also, Kent *et al.* 1994, for the construction of curvature maps based on these ideas).

Next, change coordinate systems so that the approximate tangent plane is given by the  $(x', y')$  plane in the new coordinate system and the value of  $z'$  represents the value of the surface as a function of  $x'$  and  $y'$ . Thus, the new coordinate system represents approximate Monge form at the given point.

Next, using least squares, fit a quadratic or cubic regression to  $z'$  as a function of  $x'$  and  $y'$  in this new coordinate system. The the linear terms should be approximately zero because we are in approximate Monge form; the second derivatives will therefore roughly represent the curvature information, and the third derivatives will give information about the change in principal curvature at this point.

Thus, at each of a selected number of points on the surface, we can calculate values for  $R(x, y)$ . These values can then be used in a zero crossing algorithm as described in Kent *et al.* (1996). The only complication is that although the value of  $R$  will not depend upon the coordinate system used at each point, the principal directions will be initially calculated in a local coordinate system. Therefore it is necessary to transform all the principal directions to a common coordinate system before checking for alignment. The problem of alignment of the principal directions at neighbouring points on the surface is described in Section 4 of Kent *et al.* (1996).

There are a number of issues related to the use of local regressions which need further discussion. These include the order of the polynomial to be fitted, the shape of the neighbourhood, whether or not to use weights and how big a neighbourhood to use. The laser range data are collected not as data on a square grid, but as a densely spaced set of points on vertical lines down the face with moderate gaps between these parallel vertical lines. Thus, there is a case for using elliptical neighbourhoods for the laser range data. The ellipse will be wider in the left-right direction than in the up-down direction.

Another issue concerns whether or not to use weights in the regression. Since we are looking for local behaviour of the surface near a point, it is perhaps useful to weight more highly points at the centre of the neighbourhood than points towards the edge of the neighbourhood. At the same time there is a minimum size of neighbourhood that is needed in order that fitting a cubic polynomial, say, will not be degenerate. Further, if we think of increasing the neighbourhood

size to smooth over small scale features and focus on medium scale features, it is still an open question about the best way to do this.

Another possible strategy is as follows. After switching to approximate tangent space coordinates about a point, fit successive polynomials using a sequence of increasing neighbourhoods. The first fitted polynomial will be a linear fit over a small neighbourhood. Next, fit a quadratic polynomial over a slightly larger neighbourhood but hold the linear coefficients fixed at the values given by the previous fit. Finally, fit a cubic polynomial over a still larger neighbourhood holding the linear and quadratic coefficients fixed at the previous fit. The idea behind this strategy is that lower order derivative information can be determined from a smaller sized neighbourhood than higher order information. However, more work is needed to see if this strategy is worthwhile.

### 3.3 Three-dimensional smoothing

Another approach to surface smoothing is three-dimensional smoothing. See e.g. Ayache (1995) for an overview of this approach. That is, the three dimensional image is viewed as a black and white image, black inside the object and white outside the object. This image is convolved with a Gaussian filter to smear the edge of the object. This grey-level image is then thresholded to define the smoothed surface. Algorithms such as the marching lines algorithm (Thirion and Gourdon, 1993) can then be used to pick out ridge curves on this surface. Notice that both the surface and the ridge curves are defined implicitly in this setting.

## 4 Examples and discussion

In this section, we present some ridge curves of laser range data of human faces with different amount of smoothing. With 200 manually picked landmarks, we produce a kriged surface using the conditionally positive-definite covariance function  $\sigma(\mathbf{t}) = -\|\mathbf{t}\|^5$  with quadratic drift, with different amounts of smoothing. Smoothing is controlled by a parameter  $\lambda$ ; higher  $\lambda$  introduces more smoothing and  $\lambda=0$  corresponds to an interpolating spline with no smoothing. We apply the procedure to a normal subject and to a subject with a facial abnormality, called *hemifacial microsomia*, on the left side of his face.

Fig. 1 shows the ridge curves for a smoothed kriged surface ( $\lambda=0.01$ ) projected onto the unsmoothed kriged surface. Fig. 2 shows the same ridge curves as in Fig. 1, but plotted on the smoothed surface. Fig. 3 shows the ridge curves for a smoothed surface with  $\lambda=0.05$  (the shaded surface is the smoothed surface). Black and white curves in the figures correspond to the maximal and minimal curvatures respectively.

Smoothing is necessary because small-scale features and noise on the unsmoothed kriged surface give rise to many undesirable ridge curves. Furthermore, smoothing is necessary to make the procedure more robust to the choice of landmarks. For example, the shaded surface in the bottom of Fig. 1 has ripples in the area of the lips that are artefacts of the choice of landmarks and the kriging procedure. Smoothing helps to remove such artefacts see, for example, the shaded surface at the bottom of Fig. 2.

Major features of the figures are the white midline, black nose ring, white “nostril” rings, black eye line, black lip bow-tie and black cheek lines. Each feature has a different sensitivity to the level of smoothing. The midline and the nose ring are more stable than other features like the eye line. Features like the “nostril” rings and the lip bow-tie appear to be more stable for the normal subject than for the abnormal subject. For example, the bow-tie disintegrates in the abnormal subject for  $\lambda=0.05$  in the bottom of Fig. 3. The top of Fig. 4 repeats the picture of the normal subject of the top of Fig. 1, whereas the bottom of Fig. 4 shows another normal subject with the same smoothing parameter  $\lambda=0.01$ . Notice that the basic structure of the ridge curves is similar in the two images, but there are also numerous differences in the details.

The procedure can be used to compare differences between the normal and abnormal subject. Note the left-right asymmetry of the lip bow-tie, the midline and the cheek lines in the hemifacial microsomia subject. The preservation of the asymmetry after substantial smoothing is encouraging. The question of what is the correct level of smoothing remains open.

The use of local polynomial fitting has not been very successful in practice on the laser range data. Three main problems seem to arise.

- (i) It can be a problem finding a suitable size neighbourhood for which the cubic approximation is valid.
- (ii) Moving from one point to another on the surface can involve a discontinuous change in neighbourhood, which perhaps accounts for the resulting ridge curve being rather jerky. Perhaps the Bayesian techniques of Turner and Handcock (1995) for joining patch information together will be helpful.
- (iii) Sometimes a suitable tangent plane locally is not adequate over the neighbourhood for which the cubic approximation is sought. Indeed sometimes folding can occur, i.e.  $z$  is not longer a one-valued function of  $x$  and  $y$  in this local coordinate system. An example occurs on the upper tip of the nose in the example of the human face.

This paper has concentrated on exploratory methods for identifying ridge curves. The next step is to build a formal statistical framework for comparing ridge curves from different objects.

## Acknowledgments

We are grateful to Janet West and Richard Morris for helpful discussions, and to Tricia Goodwin and Jim Moss for the data used in the example. This work was supported by an EPSRC research grant under the Stochastic Modelling in Science and Technology Programme.

## References

- Ayache, N. (1995). Medical computer vision, virtual reality and robotics-promising research tracks. *Proceedings BMVC*, pp.1-25.
- Flynn, P.J. and Jain, A.K. (1989). On reliable curvature estimation. *IEEE Computer Vision and Pattern Recognition Conference*, pp.110-116.
- Guéziec, A. (1995). Surface representation with Deformable Splines: Using Decoupled Variables. *IEEE Computational Science and Engineering*, **2**, pp.69-80.
- Kent, J.T., Mardia, K.V. and Rabe, S. (1994). Face description from laser range data. *Mathematical Methods in Medical Imaging III*. Eds. Bookstein, F.L., Duncan, J.S., Lange, N., Wilson, D.C., *SPIE Proceedings*, **2229**, pp.32-45.
- Kent, J.T., Mardia, K.V. and West, J.M. (1996). Ridge curves and shape analysis, *Proceedings BMVC '96*, to appear.
- Mardia, K.V., Kent, J.T., Goodall, C.R. and Little, J.A. (1996). Kriging and splines with derivative information. *Biometrika*, **83**, pp.207-221.
- Porteous, I.R. (1994). *Geometric Differentiation* Cambridge University Press, Cambridge.
- Thirion, J-P. and Gourdon, A. (1993). The marching lines algorithm: new results and proofs. *Research Report 1881-2 INRIA, Epidaure*.
- Turner, M. and Handcock, E.R. (1995). A Bayesian approach to 3D surface fitting and refinement. *Proceedings BMVC '95*, pp.67-76.

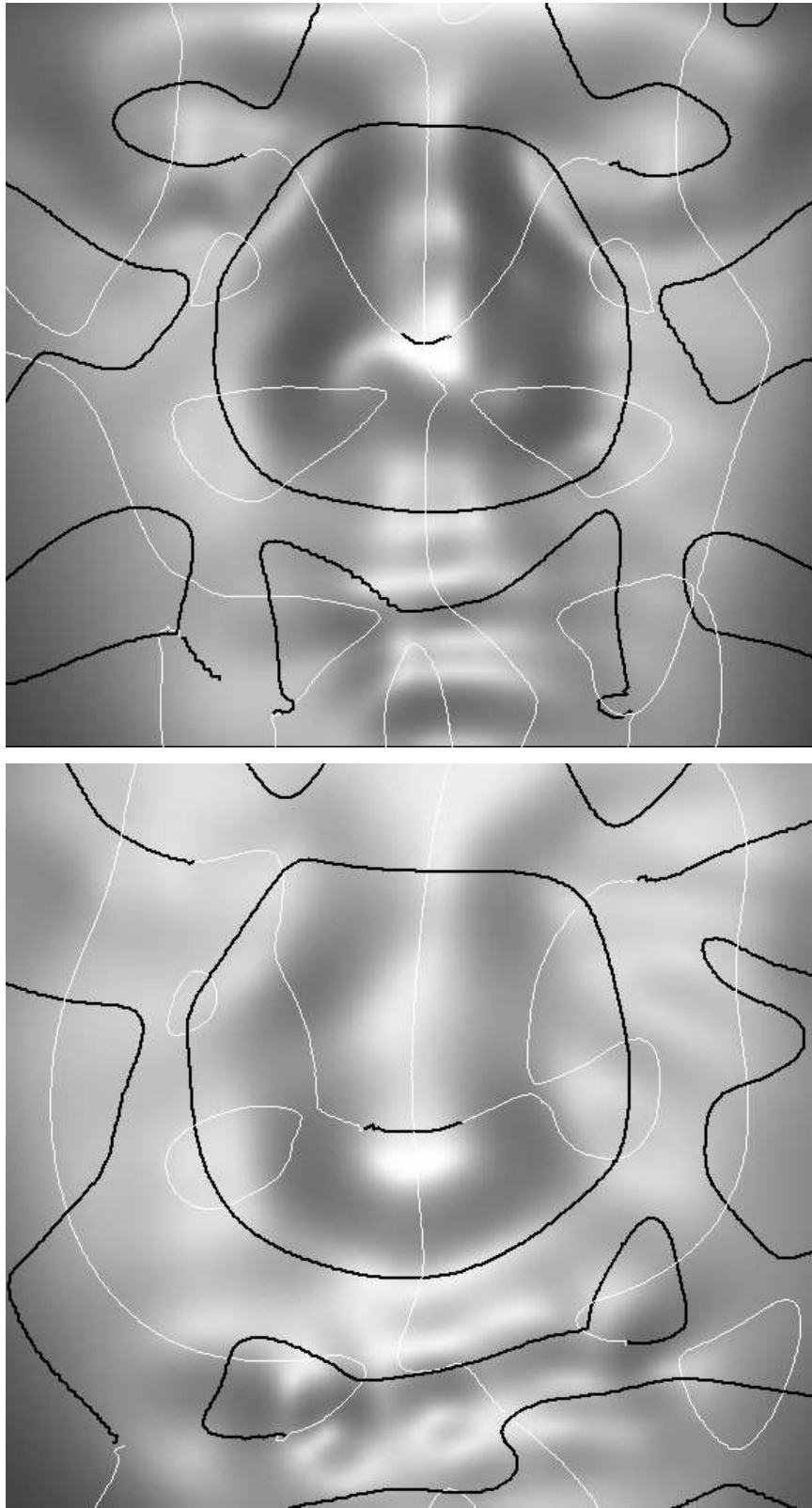


Figure 1: *Top*: Normal: ridge curves of a smoothed ( $\lambda=0.01$ ) kriged surface projected onto the unsmoothed kriged surface. *Bottom*: Hemifacial microsomia: ridge curves of a smoothed ( $\lambda=0.01$ ) kriged surface projected onto the unsmoothed kriged surface.

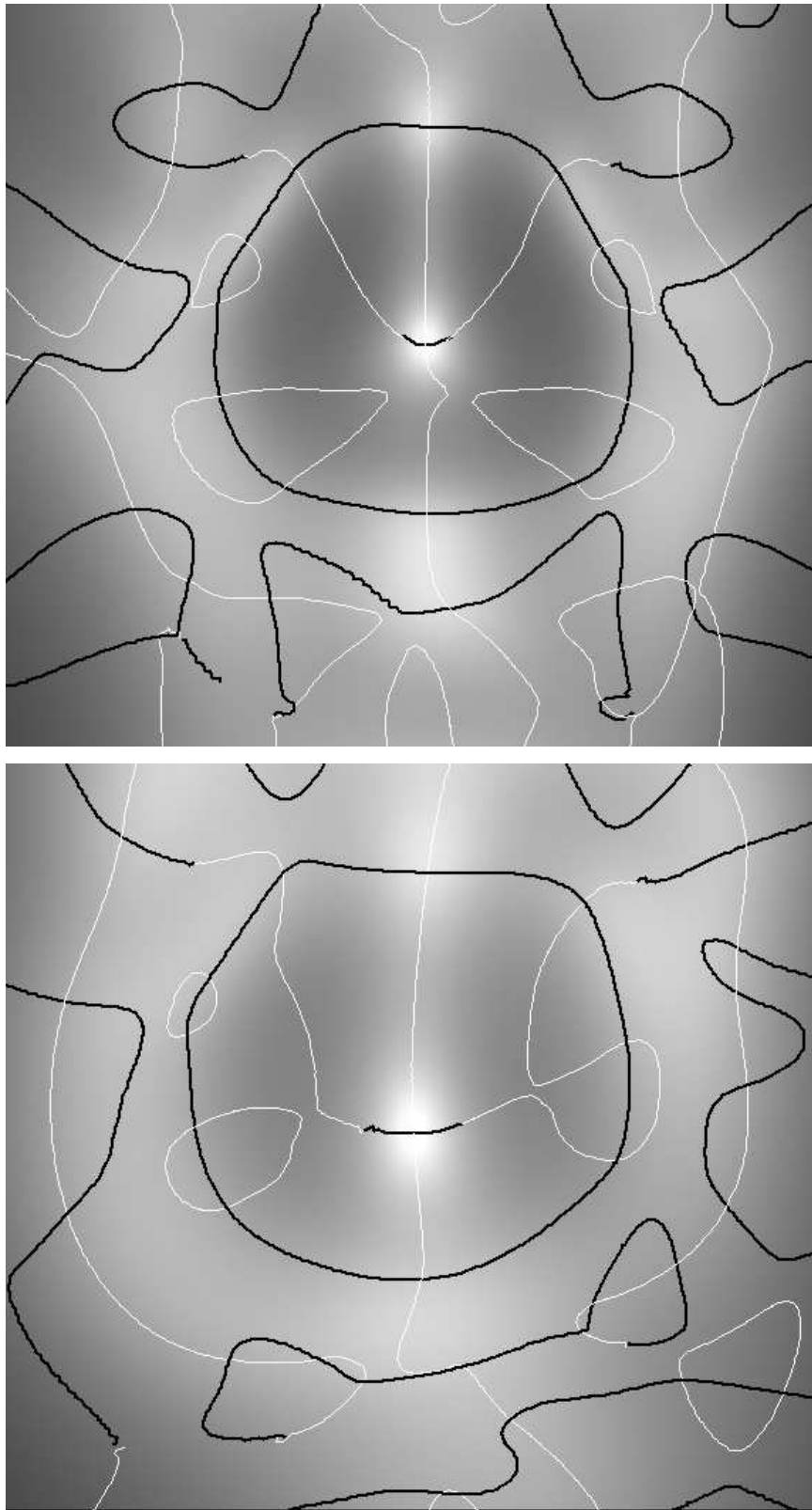


Figure 2: *Top*: Normal: ridge curves of a smoothed ( $\lambda=0.01$ ) kriged surface. *Bottom*: Hemifacial microsomia: ridge curves of a smoothed ( $\lambda=0.01$ ) kriged surface.

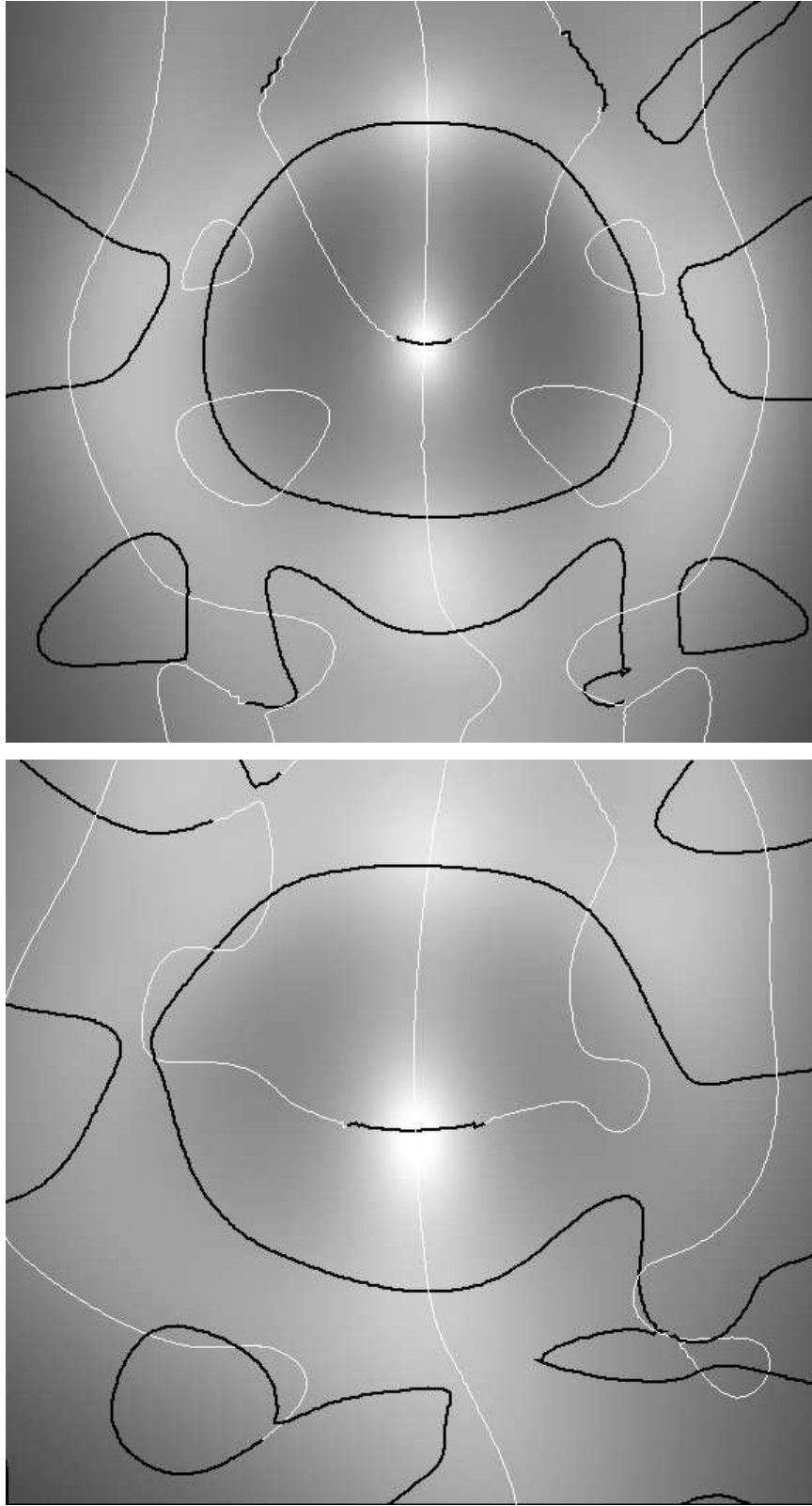


Figure 3: *Top*: Normal: ridge curves of a smoothed ( $\lambda=0.05$ ) kriged surface. *Bottom*: Hemifacial microsomia: ridge curves of a smoothed ( $\lambda=0.05$ ) kriged surface.

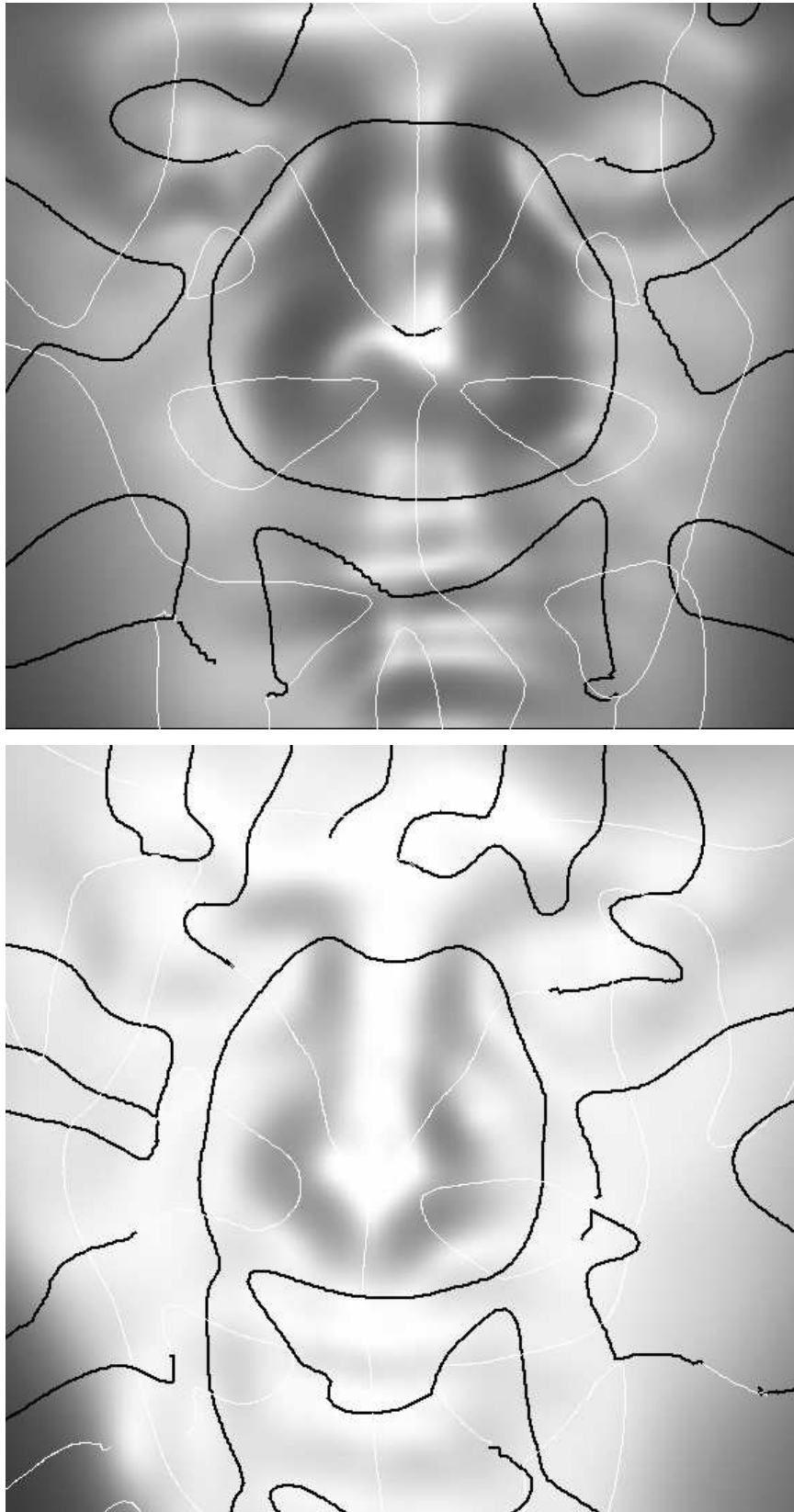


Figure 4: Ridge curves of a smoothed ( $\lambda=0.01$ ) kriged surface projected onto the unsmoothed kriged surface for two normal subjects.